

## COPY RIGHT



**ELSEVIER**  
**SSRN**

**2019IJIEMR**. Personal use of this material is permitted. Permission from IJIEMR must be obtained for all other uses, in any current or future media, including reprinting/republishing this material for advertising or promotional purposes, creating new collective works, for resale or redistribution to servers or lists, or reuse of any copyrighted component of this work in other works. No Reprint should be done to this paper, all copy right is authenticated to Paper Authors

IJIEMR Transactions, online available on 4<sup>th</sup> Sept 2019. Link

[:http://www.ijiemr.org/downloads.php?vol=Volume-08&issue=ISSUE-09](http://www.ijiemr.org/downloads.php?vol=Volume-08&issue=ISSUE-09)

Title **1Ø MULTILEVEL INVERTER TOPOLOGIES BY SELF-VOLTAGE EQUIVALENT CAPABILITIES**

Volume 08, Issue 09, Pages: 402–418.

Paper Authors

**B KARTHIK, B ANWESH KUMAR, K SATYANARAYANA**

Anu Bose Institute of Technology K.S.P Road, New paloncha, Bhadradi Kothagudem, Telangana, India



USE THIS BARCODE TO ACCESS YOUR ONLINE PAPER

To Secure Your Paper As Per **UGC Guidelines** We Are Providing A Electronic Bar Code

## 10 MULTILEVEL INVERTER TOPOLOGIES BY SELF-VOLTAGE EQUIVALENT CAPABILITIES

B KARTHIK<sup>1</sup>, B ANWESH KUMAR<sup>2</sup>, K SATYANARAYANA<sup>3</sup>

<sup>1,2,3</sup>UG Students, Dept. of Electrical and Electronics Engineering, Anu Bose Institute of Technology, K.S.P Road, New paloncha, Bhadradri Kothagudem, Telangana, India.

karthikbhukya225@gmail.com<sup>1</sup>, anweshanu291@gmail.com<sup>2</sup>, komaramsatya1999@gmail.com<sup>3</sup>

**Abstract:** In this examination, two new structures of single-stage half and half staggered both symmetrical and hilter kilter arrangements that can be utilized in drives and control of electrical machines & association of sustainable power sources. The proposed arrangement utilizes a less number of semiconductor gadgets and DC sources as contrasted and regular and recently created topologies which lead to a decrease in expense and establishment zone. The proposed topology represents an indispensable bit of leeway of self-voltage adjusting of its capacitor voltage paying little mind to load type, load elements and balance record. Additionally, the proposed topology is extended in a full manner which decreases the multifaceted nature and improves the exhibition essentially. A wide scope of correlation is finished with traditional and recently created topologies to demonstrate the predominant exhibition of proposed topologies in regards to an all out number of switches and DC sources. The multi-bearer beat width balance system is embraced for creating exchanging beats for individual switches. A lab model is produced for testing the presentation of the proposed topology for 9-level and 17-level inverters.

### 1. INTRODUCTION

Staggered inverter (MLI) gives the answer for conquer the voltage confinement of the old style 2-level inverter and to arrive at the higher power level by utilizing an arrangement association of different semiconductor gadgets with reasonable control method. The first MLI topology was presented around four decades back, and from that point forward immense push is found in the field of intensity converters and their applications [1–3]. MLI is utilized in high power applications, for example, AC engine drive [4, 5], dynamic power channels [6, 7] and reconciliation of sustainable power source into the framework [8, 9]. Aside from high-voltage similarity, MLI likewise acts advantageous advantages such like improved power quality, diminished absolute consonant twisting, less voltage

worry over the switches, great electromagnetic similarity, decreased exchanging misfortunes and dv/dt stress. Traditionally, MLIs are ordered into three classifications, and they are: full H-connect, flying capacitor and nonpartisan point braced (NPC) and these topologies are generally alluded to as 'Old style Topologies' [10, 11]. Notwithstanding, the old style topologies have a few imperatives, for example the quantity of DC sources and switches are expanded which additionally increment fringe gadgets, for example, door driver circuit, insurance circuit and warmth sink. This augmentation in the parts prompts increment in cost, by and large framework multifaceted nature, misfortunes and lessens the dependability and effectiveness of the converter. Consequently, alongside the

investigation of old style topologies, a generous push is found in the advancement of use arranged more up to date topologies with a decreased number of gadgets [12–14] and their regulation/control strategies requires a lot of bidirectional switches which increment the misfortunes in the proposed topology as contrasted and regular CHB. Additionally, the proposed topology can't be worked in an uneven mode, thus falls behind ordinary lopsided CHB. The topology of [18] at first proposes sub-MLI and after that for accomplishing a most extreme number of yield levels in a wry setup, the fell structure has been proposed. It requires an alternate assortment of switches with respect to blocking voltage capacities which increment the expense and unpredictability of the converter. Additionally, the power adjusting among various information sources is unimaginable and subsequently life is diminished. The topologies of [19, 20] utilize the arrangement association of DC sources. Likewise, a fell structure is proposed for acquiring the most extreme number of levels in yield. It requires an enormous number of bidirectional switches which expands the general misfortunes of the proposed inverter. The topologies of [17–20] experience the ill effects of one noteworthy disadvantage, for example the switches of its H-bridge need to hold up under the complete info voltage which limits the activity at higher-voltage levels. The topologies of [21–23] propose inverter which decreases switches essentially when contrasted and ordinary CHB. Notwithstanding, both double and trinary blends of DC hotspots for the hilter kilter activity of the proposed topologies are unrealistic because of which it lingers behind the regular CHB. In [24], a symmetrical topology of MLI is proposed

which decreases the quantity of segments and has a basic tweak conspire. Switches of its H-connect need to manage the full evaluated voltage of the inverter which limits its application at high-voltage levels which is a noteworthy inconvenience. In [18], another topology for MLI is proposed, however the primary downsides for this topology are the utilization of bidirectional switches, an assortment of switches and limitation on high-voltage applications. In [25], another symmetrical MLI topology has been proposed utilizing less number of switches and lessening the exchanging misfortunes up, all things considered, as contrasted and regular MLI. Be that as it may, a noteworthy disadvantage is the loss of its measured quality. The topologies of [26, 27] require more switches as contrasted and the proposed topology. In [28], topologies have been displayed for both symmetrical and hilter kilter MLIs, yet the fundamental disadvantage is the scope of accessible power factor being exceptionally thin; just loads with power factor near solidarity can be provided. In [29, 30], two topologies dependent on created H-spans are presented. The principle disadvantage of these topologies is the necessity of countless autonomous DC sources which builds the expense of these topologies. From the above writing, it is reasoned that, to accomplish a higher number of yield levels with a less number of gadgets, extraordinary trade off has been made regarding number of bidirectional switches, unidirectional switches, DC sources, assortment of switches, assortment of warmth sinks, assortment of DC sources, unwavering quality, seclusion, straightforwardness, adaptability and exchanging misfortunes. The worry referenced above has been downsized, as it were, in the proposed

topologies.

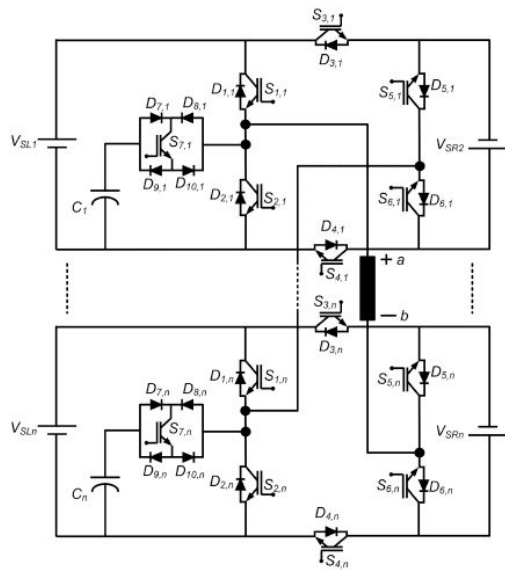


**Fig. 1-**Configuration of the proposed topology-I

**Table 1** Switching table for 9-level inverter of topology-I

Output levels	'ON' state switches	Effect on capacitor voltage	
		If ' $i_L > 0$ '	If ' $i_L < 0$ '
$C_V$	$S_4, S_6, S_7$	discharging	charging
$V_{SR}$	$S_2, S_4, S_5$	no effect	no effect
$C_V + V_{SR}$	$S_4, S_5, S_7$	discharging	charging
$V_{SL} + V_{SR}$	$S_1, S_4, S_5$	no effect	no effect
$0\text{ V}$	$S_2, S_4, S_6$	no effect	no effect
$-C_V$	$S_3, S_5, S_7$	discharging	charging
$-V_{SR}$	$S_1, S_3, S_6$	no effect	no effect
$-(V_{SL} + V_{SR} - C_V)$	$S_3, S_6, S_7$	discharging	charging
$-(V_{SL} + V_{SR})$	$S_2, S_3, S_6$	no effect	no effect

A symmetrical topology is introduced in [31] which uses single DC source in parallel of arrangement associated capacitors. The principle disservice of this topology is that solitary symmetrical setup is given. Also, four of its switches need to manage the all out voltage of the inverter limiting its application to medium voltage. The topology of [32] proposes a fell variant of the topology of [31] that can be worked at high-voltage levels as the sub-squares are associated in a fell way. In [33], the topology of [31] has been altered to lopsided form to arrive at a greatest number of yield levels. Usage of numerous bidirectional switches is the primary disadvantage of this topology. In [34], the

topology of [31] has been displayed for both symmetrical and lopsided MLIs which arrive at a higher number of yield levels. The fundamental downside is the prerequisite of an enormous number of autonomous DC sources which builds its expense tremendously. In [35], another topology of the MLI is proposed for 5-level inverter utilizing single DC source and two CHB arrangements. In this topology, capacitor voltage of one of the CHB squares is managed by a stage move balance procedure which decreases the quantity of separated DC sources considerably sum. The primary constraint of this topology is that the switches of its fundamental H-connect need to hinder the all out yield voltage of the inverter which confines its application in higher-voltage application. The topologies of [36–39] propose pressed U-cell topology which diminishes the quantity of confined DC sources by a huge edge contrasted and traditional CHB. The principle bit of leeway of these topologies is that they don't require any outside hardware for keeping up its capacitor voltage in a reasonable state. In [40], another exchanging procedure is created by consolidating particular symphonious alleviation and specific consonant disposal strategies for four leg NPC inverter which diminishes the power misfortunes, yet in addition keeps up the DC capacitors voltage in a fair state with low-voltage swells even at lower exchanging frequencies. The topology of [41, 42] proposes topologies of MLI that diminishes the DC source necessity by utilizing capacitors without the help from an outside circuit, for example the topologies of [41, 42] have self-voltage adjusting capacities, yet the two topologies require an enormous number of switches as contrasted and proposed topologies. In this paper, two new topologies are exhibited

which can be worked in both symmetrical just as deviated designs. The proposed topology has a secluded structure as it is associated in a fell manner and gives dependable activity to symmetrical and unbalanced designs with less voltage weight on the semiconductor switches. It doesn't require any outside circuit for adjusting its capacitor voltage because of its self voltage adjusting ability. 'Self-voltage adjusting' signifies the capacity of the capacitor to keep up its voltage in a decent state without requiring any guide from the outer circuit regardless of burden elements, balance file or homeless people. The symmetrical and deviated setups of proposed topologies produce the most extreme number of yield levels with less number of switches and confined DC sources relatively. The quantity of bidirectional switches additionally decreases altogether in the proposed topologies. The proposed topologies likewise have included the upside of equivalent DC source use and decreased misfortunes. A nitty gritty correlation of proposed topologies with traditional topologies and some as of late recently created topologies is done dependent on the quantity of switches and DC hotspots for both symmetrical and hilter kilter setups to viably demonstrate the advantages of the proposed topology.

## 2 Proposed MLI topologies

### 2.1 Proposed topology-I:

The summed up arrangement of topology-I in a symmetrical design is appeared in Fig. 1. Every cell in topology-I is made out of seven controlled switches, ten power diodes, two DC sources and one capacitor. The DC source on the left-hand side is numbered as VSL1, VSL2, ... , VSLn and on the right-hand side is numbered as VSR1, VSR2, ... , VSRn ('n means the quantity of arrangement cell'). The summed up numerical articulation for topology-I in the symmetrical design for 'N' cells

$$\text{number of DC sources} = 2N \quad (1)$$

$$\text{number of capacitors} = N \quad (2)$$

$$\text{number of IGBT's} = 7 \times N \quad (3)$$

$$\text{number of diodes} = 10 \times N \quad (4)$$

$$\text{number of output levels} = (8 \times N + 1) \quad (5)$$

Exchanging plan for 9-level of topology-I is given in Table 1 alongside the capacitor charging and releasing states. It must be noticed that for unadulterated resistive burden, the capacitor releases at voltage levels 'CV' and 'CV+VSR', while charging of capacitor happens at voltage level '-CV' and '(VSL+VSR-CV)'. No different states can influence the capacitor voltages. Fig. 2 shows the progression of current at all the individual levels.

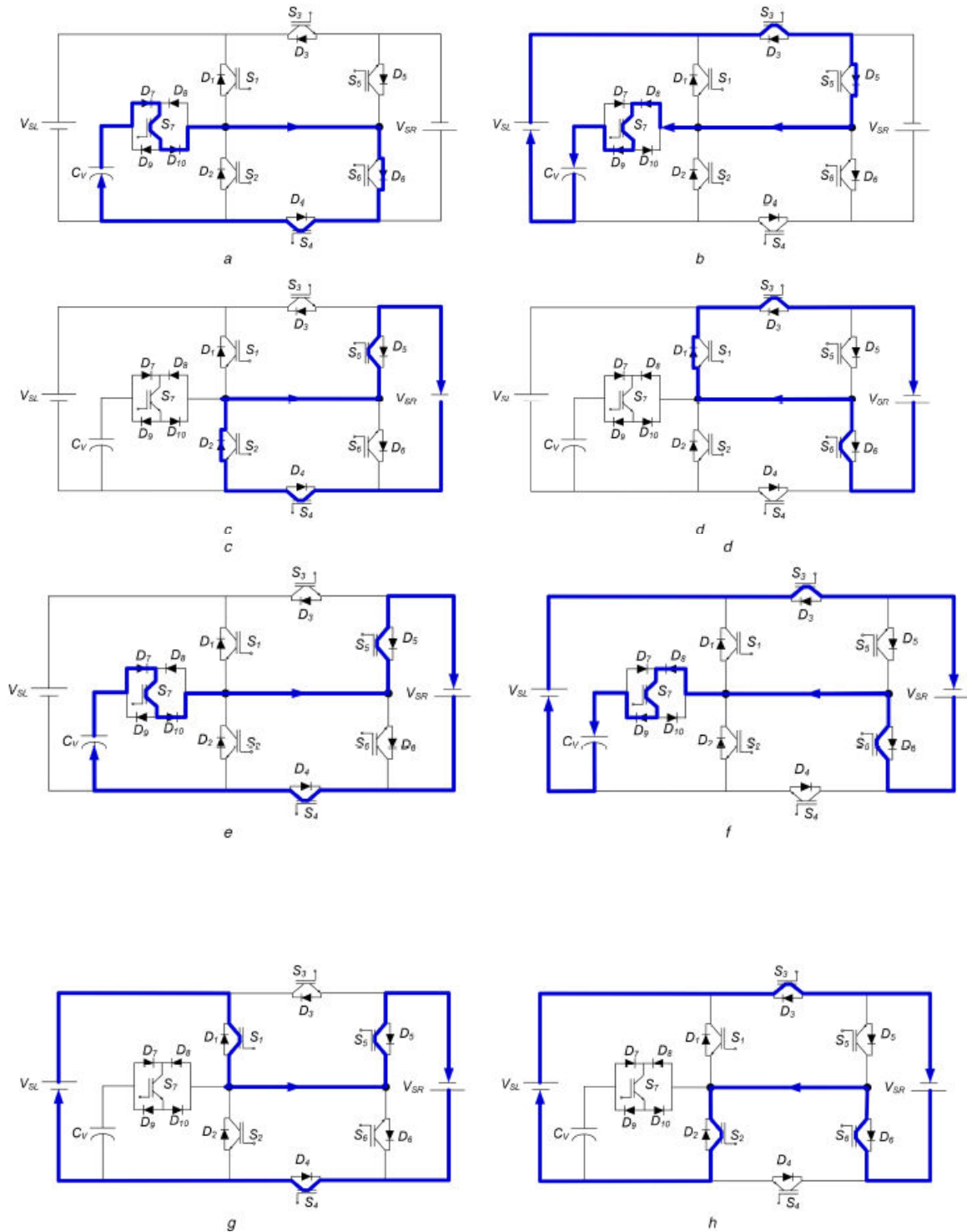


Fig. 2 Current flow direction of topology-I for 9-level output

(a) Output voltage =  $C_V$ , (b) Output voltage =  $-(V_{SL} - C_V)$ , (c) Output

voltage =  $V_{SR}$ , (d) Output voltage =  $-V_{SR}$ , (e) Output voltage =  $(V_{SR} + C_V)$ , (f) Output voltage =  $-(V_{SR}$

$+V_{SL} - C_V$ ), (g) Output voltage =  $(V_{SR}+V_{SL})$ , (h) Output voltage =  $-(V_{SR}+V_{SL})$ , (i) Output voltage =  $0V$  in every cell, and its summed up structure is given in Fig. 3 and called it as proposed topology-II. Like topology-I, the topology-II is likewise associated in a fell way to accomplish seclusion. The DC source on the left-hand side is numbered as  $V_{SL1}, V_{SL2}, \dots, V_{SLn}$  and on the right-hand side is

numbered as  $V_{SR1}, V_{SR2}, \dots, V_{SRn}$ . It can likewise be worked as symmetrical arrangement by utilizing similar estimations of DC sources. Table 2 gives the distinctive exchanging states for 9-level yield for the proposed topology-II. For topsy-turvy activity, the estimations of DC sources are allocated by Table 3. In customary lopsided CHB, the

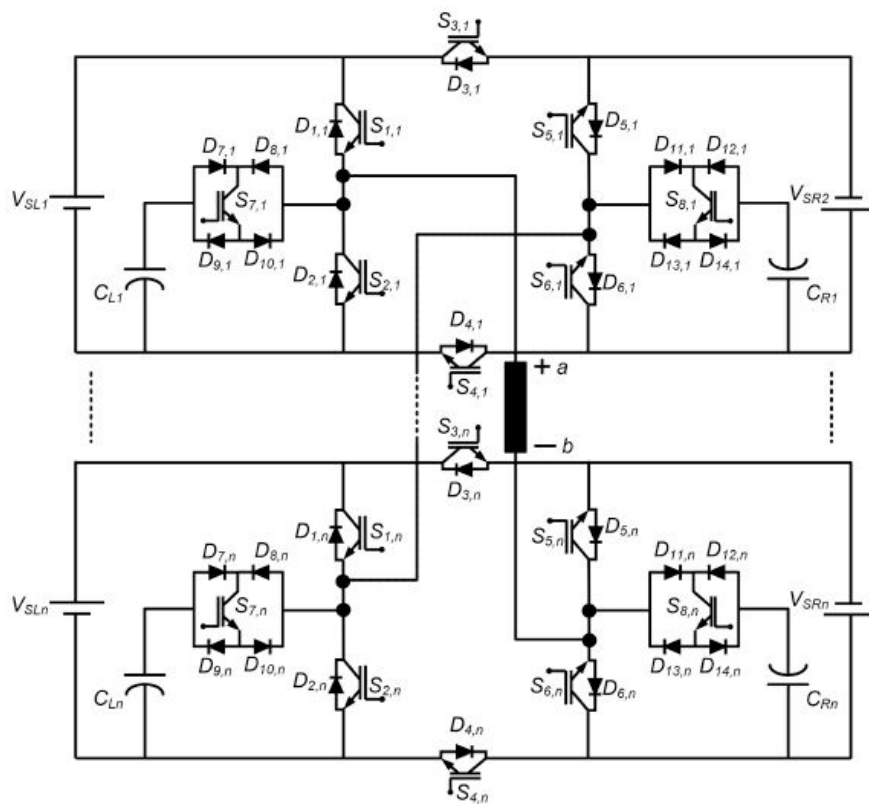


Fig. 3 Configuration of the proposed topology-II

Table 2 Switching table for 9-level inverter of topology-II

Output Levels	'ON' state switches	Effect on capacitor voltage			
		Capacitor $C_L$		Capacitor $C_R$	
		If ' $i_L > 0$ '	If ' $i_L < 0$ '	If ' $i_L > 0$ '	If ' $i_L < 0$ '
$C_L$	$S_4, S_6, S_7$	discharging	charging	no effect	no effect
$C_L + C_R$	$S_4, S_7, S_8$	discharging	charging	discharging	charging
$C_L + V_{SR}$	$S_4, S_5, S_7$	discharging	charging	no effect	no effect
$V_{SL} + V_{SR}$	$S_1, S_4, S_5$	no effect	no effect	no effect	no effect
$0V$	$S_2, S_4, S_6$	no effect	no effect	no effect	no effect
$-(V_{SL} - C_L)$	$S_3, S_5, S_7$	discharging	charging	no effect	no effect
$-(V_{SL} + V_{SR} - C_L - C_R)$	$S_3, S_7, S_8$	discharging	charging	discharging	charging
$-(V_{SL} + V_{SR} - C_L)$	$S_3, S_6, S_7$	discharging	charging	no effect	no effect
$-(V_{SL} + V_{SR})$	$S_2, S_3, S_6$	no effect	no effect	no effect	no effect

**Table 3 Realization of different levels of proposed topology-II incorporating ‘n’ number of cells**

Algorithm	Values of DC sources	Number of output levels	Configuration
first	$V_{SL1} = V_{SR1} = \dots = V_{SLn} = V_{SRn}$	$8 \times n + 1$	symmetrical
second	$\frac{V_{SL1}}{2^0} = \frac{V_{SR1}}{2^1} = \frac{V_{SL2}}{2^2} = \frac{V_{SR2}}{2^3} = \dots = \frac{V_{SLn}}{2^{2 \times n - 2}} = \frac{V_{SRn}}{2^{2 \times n - 1}}$	$4 \times [\sum_{m=1}^n (V_{SLm} + V_{SRm}) \div V_{SL1}] + 1$	asymmetrical
third	$\frac{V_{SL1}}{3^0} = \frac{V_{SR1}}{3^1} = \frac{V_{SL2}}{3^2} = \frac{V_{SR2}}{3^3} = \dots = \frac{V_{SLn}}{3^{2 \times n - 2}} = \frac{V_{SRn}}{3^{2 \times n - 1}}$	$4 \times [\sum_{m=1}^n (V_{SLm} + V_{SRm}) \div V_{SL1}] + 1$	asymmetrical
fourth	$V_{SL1} = \text{initialise}$ $V_{SR1} = 3 \times V_{SL1}$ $V_{SLn} = 4 \times \left[ \sum_{m=1}^{n-1} (V_{SLm} + V_{SRm}) \right] + V_{SL1}$ $V_{SRn} = 2 \times \left[ V_{SLn} + \left( \sum_{m=1}^{n-1} (V_{SLm} + V_{SRm}) \right) \right] + V_{SL1}$	$4 \times [\sum_{m=1}^n ((V_{SLm} + V_{SRm}) \div V_{SL1})] + 1$	asymmetrical

estimations of DC sources are doled out in a predefined way of either double (2:1) or trinary (3:1) mix and as needs be the yield levels increment. Be that as it may, some as of late distributed writing demonstrates the working of deviated topology by allocating estimations of DC sources in a predefined way of 4:1 [33], 5:1 [33] and even 7:1 [30], because of which the quantity of yield levels colossally increments as contrasted and hilter kilter CHB. Hence, so as to arrive at the most astounding number of yield levels in the proposed topology-II, another calculation is embraced which is given in Table 3 (fourth calculation).

### 2.3 Capacitor voltage balancing

In the proposed topology, the capacitor voltage consistently stays in a reasonable state independent of the heap type, balance file or burden qualities. Likewise, the proposed topology does not require any convoluted strategies for keeping up its capacitor voltage in a adjusted state. This wonder can be clarified scientifically by capacitor ampere-second equalization condition; as indicated by this condition, the net change in capacitor voltage over single exchanging cycle under enduring state condition ought to be zero. Current crosswise over capacitor is given by

$$i_C(t) = C \frac{dv_C(t)}{dt} \quad (6)$$

where ‘ $i_C$ ’ is the instantaneous capacitor current and ‘ $v_C$ ’ is the corresponding voltage across the capacitor at the same instant.

Integration of the above equation over single switching cycle yields

$$\int_0^{T_s} i_C(t) dt = C \int_0^{T_s} \left( \frac{dv_C(t)}{dt} \right) dt \quad (7)$$

$$\int_0^{T_s} i_C(t) dt = V_C(t) - V_C(0) \quad (8)$$

Presently from (8), it tends to be said that the net change in capacitor voltage over single exchanging cycle is equivalent or corresponding to vital of capacitor current over a similar exchanging cycle. In enduring state, beginning and last estimations of capacitor voltages are the equivalent. In this manner

$$\text{average capacitor current} = \frac{1}{T_s} \int_0^{T_s} i_C(t) dt = 0 \quad (9)$$

From (9), it tends to be presumed that the normal worth or DC segment of the capacitor current must be zero in harmony. The point by point examination of capacitor voltage adjusting is displayed in Fig. 4a.



### 3 Comparison studies

The proposed topology-I offers more advantages in symmetrical setup and topology-II in a deviated design. Along these lines, in this area, an appropriate correlation is drawn for topology-I in a symmetrical arrangement and topology-II is contrasted and recently created awry topologies.

#### 3.1 Comparison of symmetrical MLI

Examination of the proposed topology-I with recently created topologies of regular CHB worked in symmetrical arrangement is given in Figs. 5a and b. It very well may be seen that the proposed topology-I requires minimal measure of switches in a symmetrical setup. In addition from Fig. 5b, it very well may be seen that the DC source prerequisite in the proposed topology-I is not as much as topologies 27, 30, 34 and equivalent to topologies of [26, 32]. Henceforth, the proposed topology-I in symmetrical setup requires minimal number of gadgets as contrasted & ordinary and recently created topologies.

#### 3.2 Comparison of asymmetrical MLI

Correlation of the proposed topology-II with recently created topologies of [18, 27, 29, 30, 33, 34] and regular CHB worked in hilter kilter design is exhibited in Figs. 5c and d. It tends to be seen that the proposed topology-II requires minimal measure of switches in awry setup as contrasted and regular topology and recently created topologies. Likewise, DC source necessity is less as contrasted and CHB and the recently created topologies of [18, 27, 29, 30, 34], however requires more sources as the topology of [33] as delineated in Fig. 5d. Fig. 5 demonstrates that the proposed topologies in symmetrical and uneven setups require minimal number of gadgets (switches and DC sources) as contrasted and regular and recently created topologies. In addition, the proposed

topologies don't require any outside circuit for keeping up its capacitor voltage in a fair state. Table 4 gives the summed up correlation between the proposed topology-I and recently created topologies for 'N' number of yield levels which incorporates all out parts required for the single-stage inverter. Table 4 likewise gives the examination of different topologies dependent on all out kVA evaluations.

### 4 Simulation and experimental results

#### 4.1 Modulation scheme

For controlling the switches, the door sign are created utilizing a reasonable multi-transporter beat width tweak (MCPWM) method for both topology-I and topology-II. The transporter exchanging recurrence is kept at 100 Hz and 5 kHz, though the reference signal recurrence is kept at 50 Hz. In MCPWM procedure, the beats are produced by reasonable sensible activity among bearer and reference sign and after that the beats are bolstered to the driver circuit which enhances the size of created heartbeats to trigger the individual switch [43]. In MCPWM system, the quantity of transporter sign required is reliant on the quantity of yield levels ('M-1'). The essential methodology for MCPWM is given in Fig. 6a and entryway beats for the proposed topology-I for 9-level are given in Fig. 6b.

#### 4.2 Simulation results

To test and look at the exhibition of the proposed topologies, a recreation study has been completed utilizing MATLAB/Simulink. Topology-I is mimicked for symmetrical design as 9-level inverter and topology-II for the 17-level inverter. Diverse recreation and test parameters for both the topologies are given in Table 5. For figuring the capacitor esteem, beneath recipe is utilized:

$$C_S \geq (I_{out} \times t_{on}) / (\% \text{ripple} \times V_{in}) \quad (10)$$

where  $I_{out}$  is the current conveyed by capacitor,  $t_{on}$  is the charging/releasing time of the capacitor,  $\% ripple$  is the most extreme permissible swell substance in capacitor voltage (10% remittance is taken for proposed topologies) and  $V_{in}$  is the capacitor adjusted voltage. Fig. 7a demonstrates the reenactment consequences design under two diverse exchanging example the exchanging recurrence is all of a sudden changed from 5 kHz to 100 Hz. Fig. 7a portrays the waveforms of the yield voltage, yield current, capacitor voltage and capacitor current. From Fig. 7a, it very well may be seen that the inverter exchanging recurrence has no effect on capacitor voltage and capacitor keeps up its voltage at a fair state at both the exchanging frequencies. To look the exhibition of the

proposed topology-II in hilter kilter arrangement, 17-level yield waveforms are delineated in Fig. 7b. From the waveforms portrayed in Fig. 7b, it tends to be seen that the capacitor voltage is in a fair state at exchanging recurrence of 5 kHz. To successfully demonstrate the self-voltage adjusting of its capacitor voltage under unexpected burden change, under various modulation index and diverse reference frequencies the reproduction study is carried out dependent on 9-level inverter of topology-I and results are given in Figs. 7c and d. The working of topology-I when the sudden burden progress happens at 0.1 s is appeared in Fig. 7c. It can be seen from Fig. 7c that at 0.1 s the yield current increments;

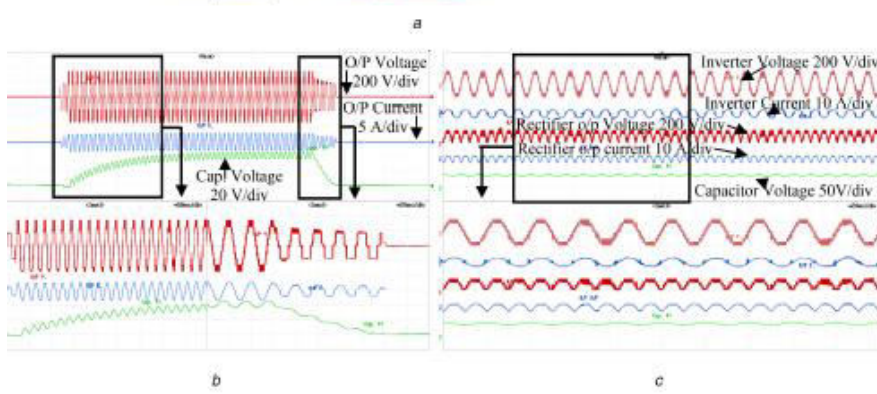
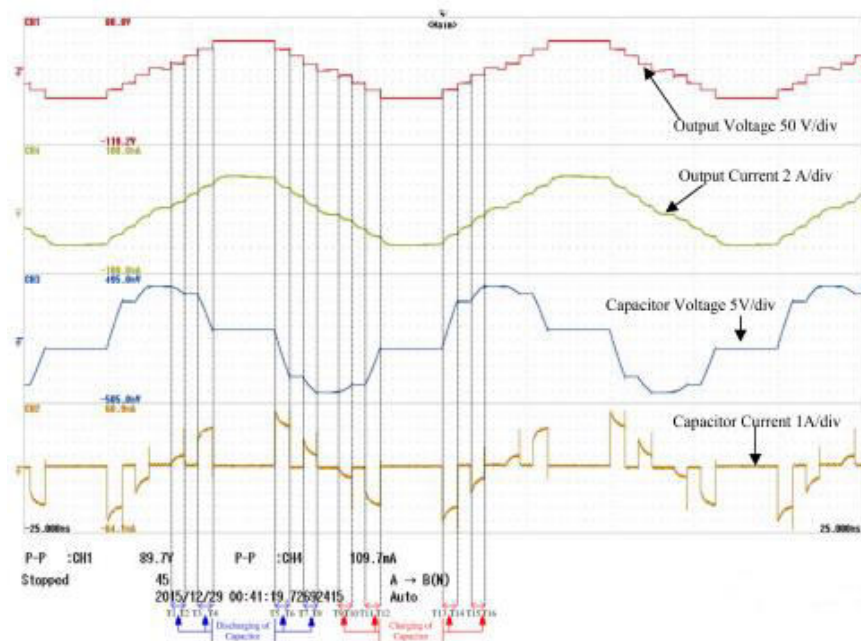


Fig.4 Experimental results for demonstrating self-voltage balancing capabilities of the proposed topology henceforth, the capacitor current likewise builds, which results in more swells in capacitor voltage, yet at the same time the voltage stays in a decent state. The working of topology-I when it is changed starting with one balance file then onto the next at 0.1s is appeared in Fig. 7d. It tends to be seen that at 0.1 s when the topology is changed solidarity adjustment file to 0.5 tweak file the yield current abatements because of which capacitor current additionally diminishes, which at last outcomes in a reduction in capacitor voltage swell, however with adjusted voltage. Consequently from Figs. 7c and d, it very well may be said that the capacitor voltage in the proposed topology consistently stays in a fair state, paying little heed to stack elements, adjustment record, exchanging recurrence or reference recurrence.

### 4.3 Experimental results

Here the definitely testing the working of proposed topologies, laboratory model has been created for the 9-/17-level inverter of topology-I & topology-II, individually. For creating the constant exchanging beats, the dSPACE1103 controller has been utilized

and the produced heartbeats are then given to door driver circuit for intensifying the created heartbeats and afterward at long last nourished to separate switches. The exploratory waveforms are dissected by the utilization of scope coder YOKOGAWA DL850E. Trial waveform, for example, yield voltage, yield current & capacitor voltages for 9-level proposed topology-I at diverse exchanging frequencies is given in Figs. 8a and b. So also, results for 17-level of topology-II are given in Figs. 8c and d. From Fig. 8, it is seen that the proposed topology functions admirably at lower just as at higher exchanging recurrence while keeping up its capacitor voltage in a fair state for both symmetrical and unbalanced configurations. To look at the charging and releasing of the capacitor voltage in the proposed inverter, a trial study has been carried out for the 9-level inverter and result is given in Figs. 4a. From Fig. 4a, it tends to be seen that the normal estimation of the capacitor current is constantly zero of every one complete cycle. Therefore, it is presumed that voltage of the capacitor consistently remains adjusted regardless of burden & tweak record.

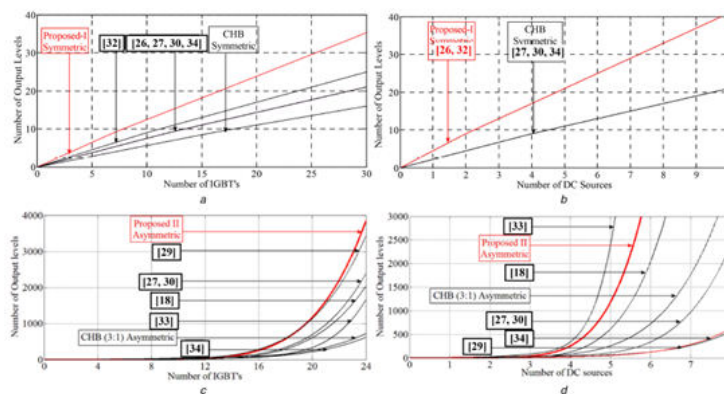


Fig. 5 Comparison of number of output levels (a) Versus number of IGBT's in symmetrical MLI, (b) Versus number of DC sources in symmetrical MLI, (c) Versus number of IGBT's in asymmetrical MLI, (d) Versus number of DC sources in asymmetrical MLI

Table 4 Generalized comparisons for single-phase symmetrical MLI

Components	MLI topology								
	Topology-I	CHB	NPC	FC	[26]	[27]	[30]	[32]	[34]
main switches	$(N+19)/4$	$2(N-1)$	$2(N-1)$	$2(N-1)$	$3(N-1)/2$	$3(N-1)/2$	$3(N-1)/2$	$5(N-1)/4$	$3(N-1)/2$
main diodes	$(N+1)$	$2(N-1)$	$2(N-1)$	$2(N-1)$	$7(N-1)/4$	$7(N-1)/2$	$3(N-1)/2$	$2(N-1)$	$3(N-1)/2$
clamping diodes	0	0	$(N-1) \times (N-2)$	0	0	0	0	0	0
DC bus capacitor/ isolated supply	$(N+3)/4$	$(N-1)/2$	$(N-1)/3$	$(N-1)/3$	$(N-1)/2$	$(N-1)/2$	$(N-1)/2$	$3(N-1)/4$	$(N-1)/2$
FC	0	0	0	$(N-1) \times (N-2)/2$	0	0	0	0	0
total number of components	$(1/2)(3N+13)$	$(9/2) \times (N-1)$	$(N-1) \times (3N+7)/3$	$(N-1) \times (3N+20)/3$	$15(N-1)/4$	$11(N-1)/2$	$4(N-1)$	$4(N-1)$	$4(N-1)$
total blocking voltage on the switches ( $V_{DC}$ as input voltage)	$(17/8) \times (N-1) \times V_{DC}$	$2 \times (N-1) \times V_{DC}$	$2 \times (N-1) \times V_{DC}$	$2 \times (N-1) \times V_{DC}$	$(9/4) \times (N-1) \times V_{DC}$	$2 \times (N-1) \times V_{DC}$	$2 \times (N-1) \times V_{DC}$	$(9/4) \times (N-1) \times V_{DC}$	$(9/4) \times (N-1) \times V_{DC}$

Additionally, a hypothetical clarification of capacitor voltage equalization should be possible from Fig. 4a. It very well may be seen that in the positive cycle the capacitor is associated in arrangement with the heap, subsequently releasing wonder happens, though in the negative halfcycle (for example T9–T10, T11–T12, T13–T14 and T15–T16) the capacitor associated arrangement with the source and henceforth charging wonder happens. Presently, the time term of charging and releasing is kept up equivalent by utilizing reasonable exchanging procedure. Consequently, net vitality got is equivalent to net vitality conveyed by a capacitor in one complete cycle. Along these lines, capacitor voltage consistently stays in a decent state. Fig. 4b demonstrates and settles at half of the information voltage, for example 45V and again returns to zero at the switch 'OFF' time. It must be noticed that the capacitors utilized in the proposed topologies set aside some effort to arrive at the relentless state condition which causes some postponement while exchanging 'ON' the inverter. This sort of postponement is likewise found in the topologies exhibited in [35–38] additionally utilizes capacitors to decrease the DC source prerequisite. In every one of these topologies, the charging and releasing

procedures are straightforwardly relative to the heap esteem, for example for the lower estimations of burden the capacitor charges rapidly & bad habit versa. To test these self-voltage adjusting abilities of the proposed inverter, it has been tried tentatively under non-straight loads, for example, diode rectifier and distinctive burden drifters and regulation records. Fig. 4c demonstrates the non-direct burden, for example diode rectifier. From Fig. 4c, it very well may be said that the capacitor voltage stays in a reasonable state under non-straight burden. Consequently, it is seen that independent of burden type, tweak record or burden elements, the capacitor voltage consistently stays in a fair state.

#### 4.4 Loss analysis and efficiency

Computation of misfortunes is extremely fundamental piece of the framework plan. MLI experiences three methods of tasks and exchanging mode. In blocking mode, the gadgets need to withstand the voltage over its terminal, consequently no present will stream in this mode over the gadget because of which the misfortunes in this mode are viewed as irrelevant. Henceforth, the larger parts of the misfortunes in MLI are in conduction and exchanging mode

$$P_{Total} = P_C + P_{SW} \quad (11)$$

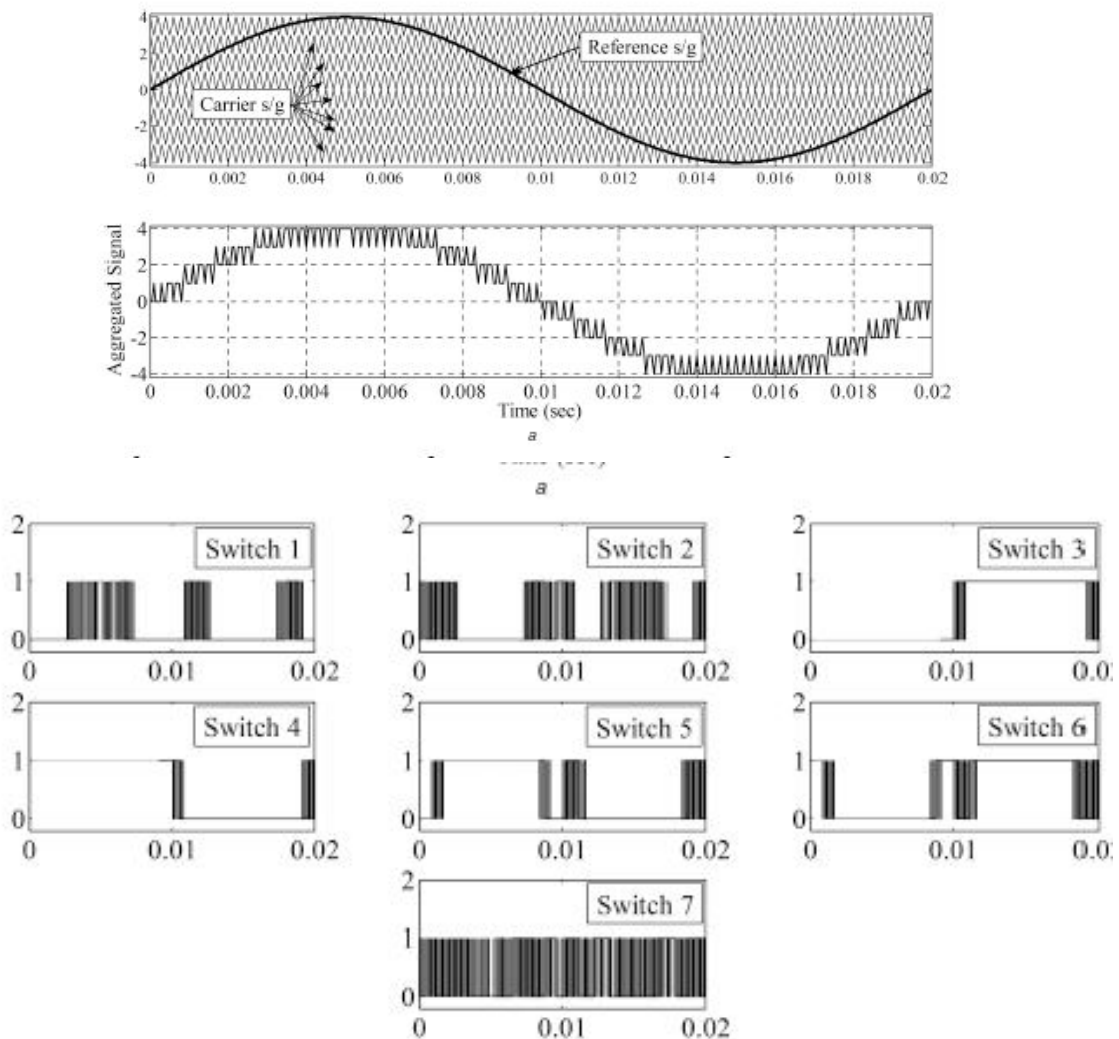


Fig. 6 Modulationscheme(a) Modulation strategies for the 9-levelMLI, (b) Gatepulses for respective switches for 9-level

**Table 5 Simulation and experimentation parameters**

Parameters	Topology-I for 9-level	Topology-II for 17-level
source-I	90 V	30 V
source-II	90 V	90 V
capacitor, $\mu\text{F}$	1200	1200
load resistance, $\Omega$	40, 80	40, 80
load inductance, mH	20, 200	20, 200
modulation index	unity, 0.5	unity
switching frequency, Hz	100 and 5000	100 and 5000

where  $P_{\text{Total}}$  is the total loss, i.e. conduction loss ( $P_C$ ) and switching loss ( $P_{\text{sw}}$ ).

#### 4.4.1 Conduction losses:

Conduction mode is depicted as the measure of intensity lost when the gadget is in 'ON' state [44]. In this paper, the two diodes and protected entryway bipolar transistors

(IGBTs) are utilized creating yield levels; subsequently, conduction misfortunes for both the gadgets are appeared. First conduction misfortunes for individual

gadgets are determined and afterward summed up to the proposed MLI. The voltage drop over an IGBT can be composed as

$$V_{CE}(i_c) = V_{CEO} + r_c \times i_c \quad (12)$$

where ' $V_{CEO}$ ' is the forward voltage drop across the IGBT, ' $r_c$ ' is the internal resistance of IGBT and ' $i_c$ ' is the collector current. The

instantaneous value of IGBT conduction losses is

$$P_{C,T}(t) = V_{CE}(t) \times i_c(t) = V_{CEO} \times i_c(t) + r_c \times i_c^2(t) \quad (13)$$

Where ' $i_{ct}$ ' is the instantaneous current. Average losses can be expressed as

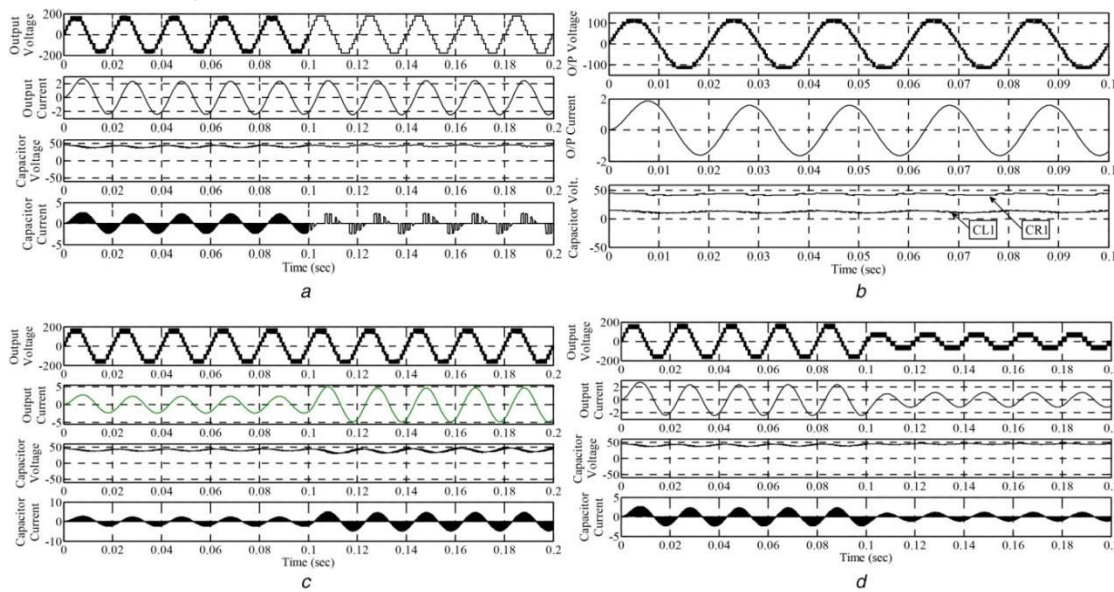


Fig. 7 Simulation results

(a) 9-Level waveforms of topology-I at two different switching frequencies of 5 kHz and 100 Hz, (b) 17-Level waveforms of topology-II at 5 kHz switching frequency, (c) Sudden load transition, (d) Sudden change in modulation index, i.e. from unity to 0.5

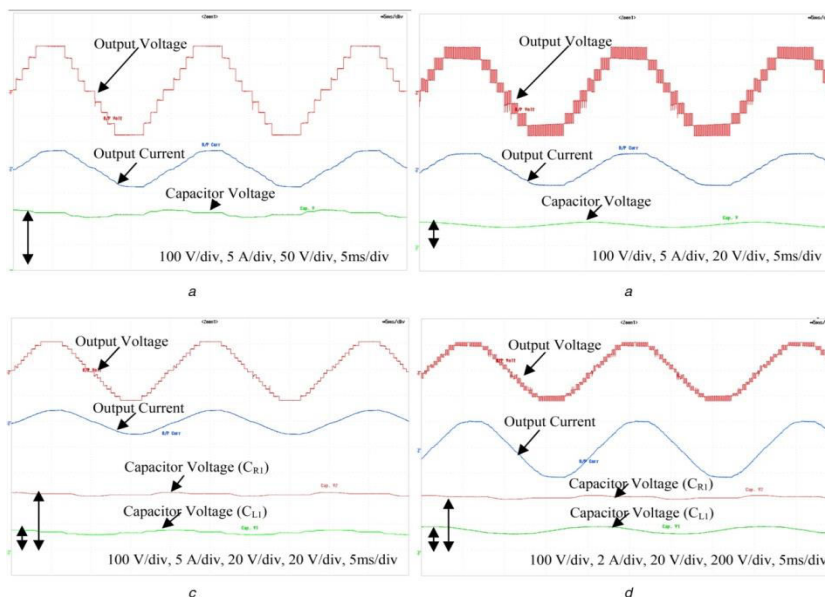


Fig. 8 Experimental results (a) 9-Level waveforms of topology-I at carrier frequency 100 Hz

b) 9-Level waveforms of topology-I at carrier frequency 5 kHz, (c) 17-Level waveforms of topology-II at carrier frequency 100 Hz, (d) 17-Level waveforms of topology-II at carrier frequency 5 kHz

$$P_{C,T} = \frac{1}{T_{SW}} \int_0^{T_{SW}} P_{C,T}(t) dt = \frac{1}{T_{SW}} \int_0^{T_{SW}} (V_{CEO} \times i_c(t) + r_c \times i_c^2(t)) dt \quad (14)$$

$$P_{C,T} = V_{CEO} \times I_{c,av.} + r_c I_{c,rms}^2 \quad (15)$$

Series	Blocking voltage, V	Current capacity, A	IGBT		Diode	
			$V_{CEO}$ , V	$r_c$ , m $\Omega$	$V_{DO}$ , V	$r_d$ , m $\Omega$
FF600R06ME3	600	600	1.9	1	1.95	0.8
FF600R12KE3	1200	600	2.15	1.25	2.5	1
FF500R25KF1	2500	500	3.6	3	2.8	1.4

**Table 7 Conduction losses for CHB**

Switch number	Conduction losses FF600R06ME3	
	IGBT, W	Diode, W
1	11.543	7.621
2	13.044	0.098
3	5.934	0.489
4	11.886	0.274
5	10.627	2.799
6	13.044	0.098
7	10.619	1.428
8	11.886	0.274
9	9.193	0.900
10	13.044	0.098
11	12.491	2.898
12	11.886	2.224
13	5.458	0.008
14	13.044	0.098
15	12.817	6.686
16	11.888	0.274
total loss	178.406	26.267

**Table 8 Conduction losses for the proposed topology-I**

Switch number	Conduction losses FF600R06ME3	
	IGBT, W	Diode, W
1	6.509	2.108
2	7.092	2.259
3	25.464	0.099
4	22.800	0.170
5	12.166	1.029
6	14.427	1.755
7	10.847	22.110
total loss	99.304	29.530

$$P_{C,D} = V_{DO} \times I_{D,av.} + r_d I_{D,rms}^2 \quad (16)$$

where ' $V_{DO}$ ' is the forward voltage drop, ' $r_d$ ' is the on-state resistance and ' $I_{D,av.}$ , ' $I_{D,rms}$ ' are the average and root-mean square (RMS) current of diode. For calculating the above-mentioned losses and to draw a suitable

comparison between CHB and proposed inverter, a MATLAB/Simulink model is built in which data provided in the datasheets are used. Specifications of MATLAB model are:

**Table 6 Forward voltage drop and internal resistance of IGBT and diode [45]**

Total input voltage: 2000 V.  
Number of DC sources: four (500V supplied by each DC source).  
Value of resistance: 100  $\Omega$ .  
Value of inductor: 100 mH.

Table 6 offers the values of the forward fall across IGBT and diodes obtained from datasheets at the side of its internal resistances for IGBT's of series FF600R06ME3 and FF500R25KF1. Table seven offers the worth of conductivity losses for CHB. Table eight offers the conductivity losses for proposed-I electrical converter. As may be seen from Tables seven and eight, conductivity losses square measure more in CHB as compared with proposed topology-I. conductivity losses square measure thirty seventh (approx.) less in proposed topology-I for each IGBT and diodes as compared with symmetrical CHB. As seen from Table eight, within the lowest voltage rated switch, i.e. S7, the foremost losses square measure within the diode; this is often as a result of the two-way switch that consists of 1 IGBT and 4 diodes. Hence, most of the losses occur

within the diode. the very best voltagerated switches havemajor losses inIGBT since the conductivity throughthe diode isnegligible.

#### 4.4.2 Switching losses:

Calculationof shift losses is complicated asno straightforward equation may be found forvoltage and current throughout a shift transient. shift lossesdepends on variety of shift transitions, i.e.transition from ‘ON’to ‘OFF’ and transition from ‘OFF’ to‘ON’, block voltagecollector current, gate resistance andjunction temperature. It conjointly depends onmodulation strategy enforced.

$$E_{\text{off},i} = \int_0^{t_{\text{off}}} v(t) \times i(t) dt = \int_0^{t_{\text{off}}} \left[ \left( \frac{V_{B,i}}{t_{\text{off}}} \times t \right) \left( -\frac{I}{t_{\text{off}}} \times (t - t_{\text{off}}) \right) \right] dt = 1/6 \times V_{B,i} \times I \times t_{\text{off}} \quad (17)$$

where  $E_{\text{off},i}$  is theenergy of the ‘ith’ switch,  $V_{B,i}$  is the blockingvoltage of the ‘ith’ switch,  $I$  is thecurrent through the ‘ith’ switchbefore turningoff and  $t_{\text{off}}$  is theturn-off time of the‘ith’ switch. mathematical expressionfor calculationof energy lossduring turn-on periodis

$$E_{\text{on},i} = 1/6 \times V_{B,i} \times I' \times t_{\text{on}} \quad (18)$$

where  $E_{\text{on},i}$  is theenergy loss of the ‘ith’ switch,  $V_{B,i}$  is theblocking voltageof the ‘ith’ switch,  $I'$  is the current throughthe ‘ith’ switchafter turningON and  $t_{\text{on}}$  is the turn-on timeof the ‘ith’ switch. Henceassuming  $I = I'$ , the total switching powerlosses forindividual switchcan becalculated as

$$P_{\text{loss},i} = (E_{\text{off},i} + E_{\text{on},i}) \times f_s = \frac{1}{6} \times V_{B,i} \times I \times (t_{\text{on}} + t_{\text{off}}) \times f_s \quad (19)$$

where  $f_s$  is the switchingfrequency of the ‘ith’ switchand  $P_{\text{loss},i}$  is thepower lossfor the ‘ith’ switch.From (19), it is clearthat

$$P_{\text{loss},i} \propto V_B \text{ and } P_{\text{loss},i} \propto f_s \quad (20)$$

As earlier mentioned thatthe obstruction voltage of the H-bridge switches utilized in several topologies hasbeen reduced to 0.5 in proposedtopology-I, therefore from (20) it's terribly clearthatthe switch losses of the

switches of H-bridge scale back to half the polygon cellin proposedtopology.To compare the switch lossesof 9-level symmetricalCHB thereupon of 9-level projected topology-I, (19) will bewrittenas

$$P_{\text{loss}} = \frac{1}{6} \times V_B \times I \times (t_{\text{on}} + t_{\text{off}}) \times f_s \quad (21)$$

Assumingthat  $t_{\text{on}}$  &  $t_{\text{off}}$  are of sameperiod and theycarry the samecurrent  $I$ , (21) can be writtenas

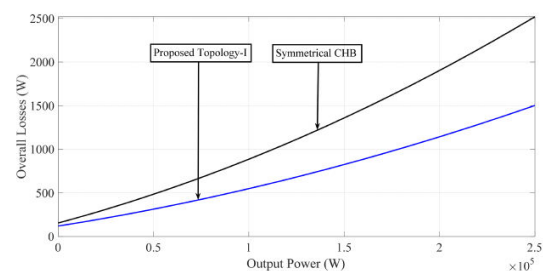


Fig. 9 Comparison of overall losses on multiple operating points

$$P_{\text{loss}} = c \times V_B \times f_s \quad (22)$$

where  $c = \frac{1}{6} \times (I \times t_{\text{on}} + t_{\text{off}})$  is a constantthus from(22) switching lossesfor 9-level symmetricalCHB having's voltagesource  $V_{DC}$  can bewrittenas

$$P_{\text{loss},9\text{-level CHB}} = 16 \times c \times V_{DC} \times f_s \quad (23)$$

Now within the projected topology-Ithere's one IGBT with obstruction avoltage of  $V_{DC}$ , fourIGBTs with obstruction voltage  $2 \times V_{DC}$  and 2 IGBTswith obstruction voltage  $4 \times V_{DC}$ . the2IGBTs with obstruction voltage  $4 \times V_{DC}$  ar switched one time throughout a basic cycleas mentioned earlier. Letthe shift frequency bedenoted by  $f_s$  and harmonic bedenoted by  $FO$ . Then by mistreatment (19), shift losses for 9-level projected inverter-I havingvoltage supply  $2V_{DC}$  will be written as



$$P_{\text{loss, 9-level Prop-I}} = c \times (V_{\text{DC}} \times f_s + 4 \times 2 \times V_{\text{DC}} \times f_s + 2 \times 4 \times V_{\text{DC}} \times f_o) \quad (24)$$

$$P_{\text{loss, 9-level Prop-I}} = 8 \times c \times V_{\text{DC}} \times \left(\frac{9}{8} \times f_s + f_o\right) \quad (25)$$

Since  $\left(\frac{9}{8} \times f_s \gg f_o\right)$ , (25) can be written as

$$P_{\text{loss, 9-level Prop-I}} = 9 \times c \times V_{\text{DC}} \times f_s \quad (26)$$

From (23) and (26)

$$P_{\text{loss, 9-level Prop-I}} \cong \frac{P_{\text{loss, 9-level CHB}}}{2} \quad (27)$$

Hence from (27), it is clear that the switching losses of the 9-level proposed inverter-I are almost half as that of 9-level symmetrical CHB under similar operating conditions.

**4.4.3 Overall losses:** In this area, a correlation has been made between the proposed topology and the regular CHB dependent on in general misfortunes and delineated in Fig. 9. For examination reason, the reenactment results have been taken in which the qualities gave in data sheets are utilized to viably figuring the general misfortunes. To demonstrate the predominance of the proposed topology over traditional CHB, the recreation results have been taken at different working focuses. From Fig. 9, it very well may be seen that the proposed topology has lower in general misfortunes as contrasted and CHB.

## 5 Conclusions

This paper proposes two new mixture topologies of symmetrical and unbalanced MLI with the self-voltage adjusting of its capacitor voltage and with a decreased number of gadgets. For acquiring the most extreme number of yield levels in a wry arrangement, another calculation is proposed. The proposed topologies have been tried tentatively for 9-level and 17-level inverters under various exchanging frequencies. For successfully exhibiting the self-voltage adjusting wonder of capacitor voltage, the proposed topologies have been tried under non-straight burden,

responsive burden, under various balance file and diverse burden progress. A wide scope of correlation is drawn between the proposed topologies, ordinary and the recently created topologies which demonstrate that the proposed topologies require minimal number of switches and DC sources as contrasted and different topologies.

## 6 REFERENCES

1. Akagi, H.: 'Order, wording, and utilization of the measured staggered course converter (MMCC)', *IEEE Trans Power Electron.*, 2011, 26, (11), pp. 3119–3130
2. Liu, C.-H., Hsu, Y.-Y.: 'Plan of a self-tuning PI controller for a STATCOM utilizing molecule swarm advancement', *IEEE Trans Ind Electron.* 2010, 57, (2), pp. 702–715
3. Ristow, A., Begovic, M., Pregelj, An, et al.: 'Advancement of a technique for improving photovoltaic inverter unwavering quality', *IEEE Trans. Ind. Electron.*, 2008, 55, (7), pp. 2581–2592
4. Hagiwara, M., Nishimura, K., Akagi, H.: 'A medium-voltage engine drive with a secluded staggered PWM inverter', *IEEE Trans Power Electron.* 2010, 25, (7), pp. 1786–1799
5. Franquelo, L.G., Rodriguez, J., Leon, J.I. et al.: 'The time of staggered converters arrives', *IEEE Ind Electron Mag.*, 2008, 2, (2), pp. 28–39
6. Cheng, Y., Qian, C., Crow, M.L. et al.: 'A correlation of diode-clamped and full staggered converters for a STATCOM with vitality stockpiling', *IEEE Trans. Ind. Electron.*, 2006, 53, (5), pp. 1512–1521
7. Barrena, J.A., Marroyo, L., Vidal, M.A.R., et al.: 'Singular voltage adjusting procedure for PWM full H-connection converter-based STATCOM', *IEEE Trans Ind. Electron.*, 2008, 55, (1), pp. 21–29

8. Alepuz, S., Buquets-Monge, S., Bordonau, J., et al.: 'Interfacing sustainable power source to the utility matrix utilizing a three-level inverter', *IEEE Trans. Ind Electron* 2006, 53, (5), pp. 1504–1511
9. Walker, G., Sernia, P.: 'Full DC–DC converter association of photovoltaic modules', *IEEE Trans. Power Electron.*, 2004, 19, (4), pp. 1130–1139
10. Nami, A., Zare, F., Ghosh, A., et al.: 'A half and half bridge converter topology with arrangement associated symmetrical and lopsided diode-braced H-connection cells', *IEEE Trans Power Electron.*, 2011, 26, (1), pp. 51–65
11. Veenstra, M., Rufer, A.: 'Control of a half and half lopsided staggered inverter for focused medium-voltage modern drives', *IEEE Trans Ind Appl.*, 2005, 41, (2), pp. 655–664.